

THIS REPORT HAS BEEN DELIMITED
AND CLEARED FOR PUBLIC RELEASE
UNDER DOD DIRECTIVE 5200.20 AND
NO RESTRICTIONS ARE IMPOSED UPON
ITS USE AND DISCLOSURE.

DISTRIBUTION STATEMENT A

APPROVED FOR PUBLIC RELEASE;
DISTRIBUTION UNLIMITED.

428432

SURFACE WAVES ON A UNIAXIAL PLASMA SLAB;
THEIR GROUP VELOCITY AND POWER FLOW

by

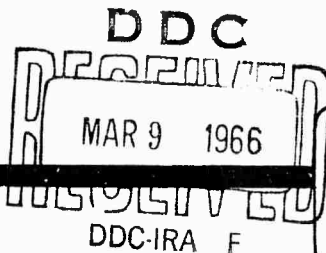
H. L. Bertoni and A. Hessel

Research Report No. PIBMRI-1294-65
Contract No. NONR 839(38)

Sponsored by
Advanced Research Projects Agency

Monitored by
Office of Naval Research
Washington, D. C.

October 12, 1965



POLYTECHNIC INSTITUTE OF BROOKLYN
MICROWAVE RESEARCH INSTITUTE

Electrophysics Department

ARPA Order No. 529

Research Report No. PIBMRI-1294-65
Contract No. NONR 839(38)

SURFACE WAVES ON A UNIAXIAL PLASMA SLAB;
THEIR GROUP VELOCITY AND POWER FLOW

by

H. L. Bertoni and A. Hessel

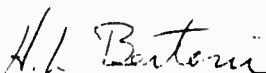
Polytechnic Institute of Brooklyn
Electrophysics Department

Graduate Center
Route 110
Farmingdale, New York 11735

Research Report No. PIBMRI-1294-65
Contract No. NONR 839(38)

October 12, 1965

Title Page
Acknowledgement
Summary
Table of Contents
20 Pages of Text
References



H. L. Bertoni



A. Hessel



Herbert J. Carlin
Head of Department

Reproduction in whole or in part is permitted for
any purpose of the United States Government.

Sponsored by

Advanced Research Projects Agency

Monitored by

Office of Naval Research
Washington, D. C.

ACKNOWLEDGEMENT

This research was supported by the Office of Naval Research, Washington, D. C. , under Contract No. NONR 839(38). ARPA Order No. 529.

SUMMARY

The relation between group velocity and the velocity of energy transport for surface waves in plane-stratified, anisotropic, dispersive media, which was derived in (1), is verified by direct calculation for the case of surface waves on a uniaxial, cold plasma slab located in free space. A superimposed D. C. magnetic field of infinite strength and parallel to the interfaces generates the uniaxial anisotropy in the slab. Surface waves having an arbitrary direction of propagation with respect to the D. C. magnetic field are considered. A useful graphical presentation of the dispersion relation is given, from which the direction of propagation of "surface wave rays" is directly obtained.

This research was supported by the Office of Naval Research, Washington, D. C., under Contract No. NONR 839(38). ARPA Order No. 529.

TABLE OF CONTENTS

	Page
ACKNOWLEDGEMENT	ii
SUMMARY	iii
TABLE OF CONTENTS	iv
INTRODUCTION	1
FIELDS AND DISPERSION RELATION	1
PROPERTIES OF THE DISPERSION RELATION	7
GROUP VELOCITY AND ENERGY TRANSPORT VELOCITY	15
APPENDIX	18
REFERENCES	20

INTRODUCTION

The group velocity of a surface wave propagating in a plane-stratified, anisotropic, dispersive medium that is also linear and lossless has been shown to be equal to the velocity of energy transport of the surface wave as a whole.⁽¹⁾ This velocity is defined as the integral of the real part of the Poynting vector over the coordinate in the direction of stratification divided by the integral of the stored energy density over this coordinate. In this paper the above relation is verified by direct calculation for the case of surface waves supported by a uniaxial, cold-electron plasma slab. The plasma slab is assumed to be of infinite extent and to be located in free space. A static magnetic field of infinite strength and parallel to the interfaces between the plasma and free space generates the anisotropy.

The characteristics of trapped surface waves propagating on anisotropic plasma slabs have been discussed in the literature for various specific directions of propagation relative to the static magnetic field. Wait⁽²⁾ has considered the surface waves propagating on a thin plasma slab with an arbitrary static magnetic field. Requiring the plasma slab to be thin reduces the effect of the static magnetic field to that which would be produced by the component normal to the slab alone. Meltz and Shore⁽³⁾ discuss the excitation of surface waves on a slab of arbitrary thickness when the static magnetic field is perpendicular to the slab and of infinite strength. In both of these cases, the anisotropy is such that the slab configurations have rotational symmetry about the coordinate normal to the slab and hence the characteristics of the surface waves will be independent of the direction of propagation. Furthermore, as in isotropic slab configurations, the velocity of energy transport of surface waves on these slab configurations will be parallel to the transverse wave vector.

When the static magnetic field is parallel to the air-plasma interfaces, the effect of the resultant anisotropy is more striking since then the characteristics of the surface waves on the slab depend on their directions of propagation with respect to the static magnetic field. Also, the velocity of energy transport will not be parallel, in general, to the transverse wave vector. Examples found in the literature, of surface waves on slab configurations with axis of anisotropy parallel to the interfaces, do not illustrate these anisotropic effects as they are restricted either to propagation along^(3, 4, 5) or normal⁽⁶⁾ to the static magnetic field. In either case, the velocity of energy transport is parallel to the transverse wave vector. In this paper, however, the surface wave fields are considered for arbitrary directions of propagation with respect to the static magnetic field of infinite strength. It will be shown that for this configuration, the velocity of energy transport of each surface wave is not parallel, in general, to the transverse wave vector, and that the direction, as well as the magnitude, of the real part of the complex Poynting vector varies

with the coordinate normal to the slab. Thus the slab configuration provides a non-trivial example of the equality of the surface wave's group velocity and its energy transport velocity. The excitation of the surface waves is not considered here.

In the first section of this paper the fields and dispersion relation of the E-type surface waves, which have no component of R. F. magnetic field along the static magnetic field, are found. A graphical procedure for solving the dispersion relation and the properties of the dispersion curves are discussed in the second section. The last section is devoted to an analytical verification of the equality of group velocity and energy transport velocity for the surface waves. The Appendix contains a proof that the uniaxial slab configuration can support only the E-type surface waves described in the body of the paper.

FIELDS AND DISPERSION RELATION

In this section, the fields and dispersion relation for surface waves on a uniaxial electron plasma slab are found. The plasma within the slab is homogeneous and the superimposed D. C. magnetic field, which is assumed to be of infinite strength, is parallel to the y axis (see Fig. 1). In the linear or small signal approximation, the interaction of the uniaxial plasma with a monochromatic electromagnetic field may be described by a relative dielectric tensor $\underline{\epsilon}'$. Neglecting collision loss, when the D. C. magnetic field is in the y direction, $\underline{\epsilon}'$ takes the form^(3, 4)

$$[\underline{\epsilon}'] = \begin{bmatrix} 1 & 0 & 0 \\ 0 & 1-X & 0 \\ 0 & 0 & 1 \end{bmatrix} \quad (1)$$

where $X = (\omega_p/\omega)^2$ and ω_p is the electron plasma frequency. Thus in the plasma slab $\underline{\epsilon} = \epsilon_0 \underline{\epsilon}'$ while in the air regions $\underline{\epsilon} = \epsilon_0 \underline{1}$, where $\underline{1}$ is the unit dyadic. The permeability tensor $\underline{\mu}$ is given everywhere by $\underline{\mu} = \mu_0 \underline{1}$.

The surface wave fields, which decay exponentially in the air regions, have transverse dependence $e^{-j(k_x x + k_y y)}$, k_x and k_y being real transverse wave numbers. These fields will be constructed from those plane wave solutions appropriate to the plasma region and those appropriate to the free space regions. The plane wave solutions appropriate to the plasma slab are those waves of the form

$$\left. \begin{array}{l} \underline{E}(\underline{r}, \underline{k}) \\ \underline{H}(\underline{r}, \underline{k}) \end{array} \right\} = \left\{ \begin{array}{l} \underline{e}'(\underline{k}) \\ \underline{h}'(\underline{k}) \end{array} \right\} e^{-j\underline{k} \cdot \underline{r}} \quad (2)$$

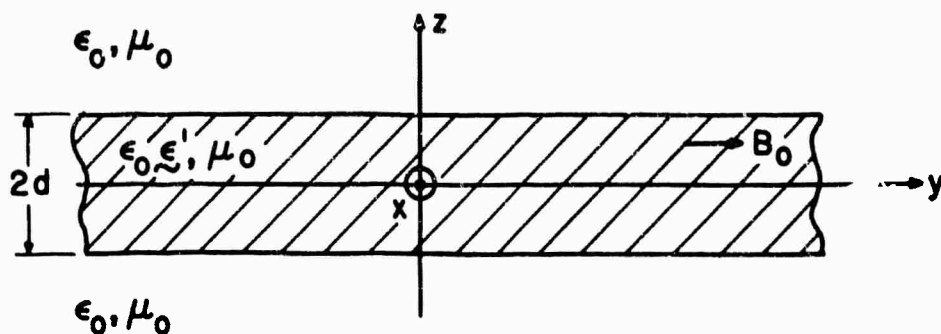


Fig. 1 Physical Configuration of the Anisotropic Plasma Slab.

which can propagate in an infinite homogeneous plasma described by the relative dielectric tensor $\underline{\epsilon}'$ given in (1). Similarly, the plane wave solutions appropriate to the free space are those having the form given in (2) which can exist when the plasma slab is absent.

The plasma plane waves are found by substituting \underline{E} and \underline{H} from (2) into Maxwell's equations. The resultant equations are, when the time dependence $e^{j\omega t}$ is suppressed,

$$\left. \begin{aligned} \underline{k} \times \underline{e}' &= \omega \mu_0 \underline{h}' \\ \underline{k} \times \underline{h}' &= -\omega \epsilon_0 \underline{\epsilon}' \cdot \underline{e}' \end{aligned} \right\} \quad (3)$$

Multiplying the first equation by $\underline{k} \times$ and substituting the second gives $\underline{k} \times (\underline{k} \times \underline{e}') = -k_0^2 \underline{\epsilon}' \cdot \underline{e}'$ with $k_0^2 = \omega^2 \epsilon_0 \mu_0$. Expanding the triple cross-product, this equation may be written in dyadic form as

$$(k_0^2 \underline{\epsilon}' + \underline{k} \underline{k} - k^2 \underline{1}) \cdot \underline{e}' = 0, \quad (4)$$

which is equivalent to three homogeneous equations in three unknowns. For there to be non-trivial solutions of (4), the determinant of the matrix representation of the dyadic operator $(k_0^2 \underline{\epsilon}' + \underline{k} \underline{k} - k^2 \underline{1})$ must vanish. Letting $\underline{k} = \underline{k}_t + \underline{z}_0 k_z$, with $\underline{k}_t = \underline{x}_0 k_x + \underline{y}_0 k_y$, the

vanishing of the determinant results in the plane wave dispersion relation $D_p(\underline{k}, \omega) = 0$ for an infinitely extended, homogeneous, uniaxial plasma. This plane wave dispersion relation may be solved for κ . Four solutions result, which are

$$\kappa = \left\{ \begin{array}{l} \pm \sqrt{k_o^2 - k_t^2} \\ \pm \sqrt{(1-X)(k_o^2 - k_y^2) - k_x^2} \end{array} \right\}. \quad (5)$$

The sign choice before each root refers to waves carrying power or decaying in the positive or negative z direction. Substituting each of the four solutions given in (5) into (4), the corresponding field vector \underline{e}' can be found. Finally, the pertinent \underline{h}' can be calculated from (3).

The above method may be repeated to find the plane wave fields \underline{e}'_a and \underline{h}'_a for free space. Since \underline{k}_t must be the same for the entire surface wave if the transverse fields are to be continuous everywhere across the planes $z = \pm d$, it follows that the free space wave vector $\underline{k}_a = \underline{k}_t + \underline{z}_o \kappa_a$. Substituting the form of \underline{E} and \underline{H} given in (2) into Maxwell's equations for free space gives

$$\left. \begin{array}{l} \underline{k}_a \times \underline{e}'_a = \omega \mu_o \underline{h}'_a \\ \underline{k}_a \times \underline{h}'_a = -\omega \epsilon_o \underline{e}'_a \end{array} \right\}. \quad (6)$$

From (6), the homogeneous equations that determine \underline{e}'_a are found, in dyadic form, to be

$$[(k_o^2 - k_a^2) \underline{1} + \underline{k}_a \underline{k}_a] \cdot \underline{e}'_a = 0. \quad (7)$$

From the requirement that the determinant of the matrix representation of $[(k_o^2 - k_a^2) \underline{1} + \underline{k}_a \underline{k}_a]$ vanish for non-trivial solutions of \underline{e}'_a to exist, one can solve for κ_a as

$$\kappa_a = \pm \sqrt{k_o^2 - k_t^2}. \quad (8)$$

When these values of κ_a are used, (7) reduces to $\underline{k}_a \cdot \underline{e}'_a = 0$, i. e., the plane wave electric field is orthogonal to the wave vector \underline{k}_a , a condition that does not uniquely determine \underline{e}'_a . Commonly chosen solutions for \underline{e}'_a are those corresponding to TM and TE modes with respect to the z direction. Other possible choices for \underline{e}'_a , which will

prove more useful in this analysis, are those of the so-called E-type and H-type modes, which are appropriate linear combinations of the TM and TE modes. The E-type modes with respect to y are characterized by the vanishing of the y component of the magnetic field, while the H-type modes are characterized by the vanishing of the y component of the electric field.

In each region, the surface wave fields will be a combination of the plane wave solutions appropriate to that region, the relative amplitudes of which can be found from the radiation condition and the continuity conditions at $z = \pm d$. Since the free space outside the slab is homogeneous, the surface waves are characterized by an exponential decay of their fields away from the slab. Such decay requires that κ_a be imaginary and that for Region 1 the sign choice in (8) be taken to give $\kappa_a = -j|\kappa_a|$, so that the fields will decay in the positive z direction. For the plane waves in Region 3, the sign must be taken so as to give $\kappa_a = j|\kappa_a|$, which will result in fields that decay in the negative z direction.

It will be shown later that a surface wave, whose fields in the plasma slab are a combination of those plane wave fields corresponding to $\kappa = \pm \sqrt{(1-X)(k_o^2 - k_y^2) - k_x^2}$, exists only for $X > 1$. In the Appendix it is shown that H-type surface wave modes, characterized by the vanishing of the y component of the electric field, cannot propagate on the uniaxial plasma slab. The plane wave fields in the plasma region corresponding to $\kappa = \pm \sqrt{(1-X)(k_o^2 - k_y^2) - k_x^2}$ are E-type modes and have the form

$$\left. \begin{aligned} \underline{e}' &= A[\underline{x}_o k_x k_y - \underline{y}_o (k_o^2 - k_y^2) + \underline{z}_o k_y \kappa] \\ \underline{h}' &= A \omega \epsilon_o [\underline{x}_o \kappa - \underline{z}_o k_x] \end{aligned} \right\} \quad (9)$$

with A an arbitrary constant.

As mentioned earlier, the only requirement on \underline{e}'_a is that $\underline{k}_a \cdot \underline{e}'_a = 0$. Hence, we may arbitrarily select the transverse part of \underline{e}'_a and then use the requirement $\underline{k}_a \cdot \underline{e}'_a = 0$ to find the corresponding z component of \underline{e}'_a . A particularly useful form of the transverse part of \underline{e}'_a is obtained by choosing it to be identical with the transverse part of \underline{e}' as given in (9). This choice will be seen to simplify the application of the continuity requirement on the transverse fields at $z = \pm d$. Following this procedure one finds

$$\left. \begin{aligned} \underline{e}'_a &= B[\underline{x}_o k_x k_y - \underline{y}_o (k_o^2 - k_y^2) + \underline{z}_o k_y \kappa_a] \\ \underline{h}'_a &= B \omega \epsilon_o [\underline{x}_o \kappa_a - \underline{z}_o k_x] \end{aligned} \right\} \quad (10)$$

with B an arbitrary constant. It is seen that the transverse part of \underline{h}'_a has the same vector direction as the transverse part of \underline{h}' . It will thus be possible to satisfy the continuity conditions at $z = \pm d$ using only the plane waves exhibited in (9) and (10).

Since the wave number κ_a must be imaginary, let

$$\alpha = \sqrt{k_t^2 - k_o^2} \quad (11)$$

so that $\kappa_a = \pm j\alpha$ where α is real and positive. Then in Region 1, $\kappa_a = -j\alpha$, for decay in the positive z direction, and if $\underline{\rho} = \underline{x}_o x + \underline{y}_o y$, the fields are

$$\left. \begin{aligned} \underline{E} &= B_1 [\underline{x}_o k_x k_y - \underline{y}_o (k_o^2 - k_y^2) - \underline{z}_o j k_y \alpha] e^{-\alpha z} e^{-j \underline{k}_t \cdot \underline{\rho}} \\ \underline{H} &= B_1 \epsilon_o [-\underline{x}_o j \alpha - \underline{z}_o k_x] e^{-\alpha z} e^{-j \underline{k}_t \cdot \underline{\rho}} \end{aligned} \right\} \quad (12)$$

while in Region 3, $\kappa_a = j\alpha$, and the corresponding fields are

$$\left. \begin{aligned} \underline{E} &= B_3 [\underline{x}_o k_x k_y - \underline{y}_o (k_o^2 - k_y^2) + \underline{z}_o j k_y \alpha] e^{\alpha z} e^{-j \underline{k}_t \cdot \underline{\rho}} \\ \underline{H} &= B_3 \epsilon_o [\underline{x}_o j \alpha - \underline{z}_o k_x] e^{\alpha z} e^{-j \underline{k}_t \cdot \underline{\rho}} \end{aligned} \right\} \quad (13)$$

The constants B_1 and B_3 have yet to be determined.

For simplicity in what follows, we define β as

$$\beta = \sqrt{(1-X)(k_o^2 - k_y^2) - k_x^2} \quad (14)$$

so that in (5) $\kappa = \pm \beta$. It will be shown that for a surface wave to propagate on the slab β must be real. The fields in Region 2 will be the sum of the fields of the two plane waves having the vector form displayed in (9) and traveling in opposite directions along z . The most general form of such a sum is

$$\underline{E} = \left\{ [\underline{x}_o k_x k_y - \underline{y}_o (k_o^2 - k_y^2)] (A_1 e^{-j\beta z} + A_2 e^{j\beta z}) + \underline{z}_o k_y \beta (A_1 e^{-j\beta z} - A_2 e^{j\beta z}) \right\} e^{-j \underline{k}_t \cdot \underline{\rho}} \quad (15-a)$$

and

$$\underline{H} = \epsilon_o \left\{ \underline{x}_o \beta (A_1 e^{-j\beta z} - A_2 e^{j\beta z}) - \underline{z}_o k_x (A_1 e^{-j\beta z} + A_2 e^{j\beta z}) \right\} e^{-j \underline{k}_t \cdot \underline{\rho}} \quad (15-b)$$

with A_1 and A_2 to be determined from the boundary conditions at $z = \pm d$.

Requiring \underline{E}_t and \underline{H}_t to be continuous at $z = \pm d$ results in four homogeneous equations in four unknowns from which the relative amplitudes as well as the surface wave dispersion relation can be found. The continuity conditions at $z = d$ given the equations

$$\left. \begin{aligned} B_1 e^{-\alpha d} &= A_1 e^{-j\beta d} + A_2 e^{j\beta d} \\ -j\alpha B_1 e^{-\alpha d} &= \beta (A_1 e^{-j\beta d} - A_2 e^{j\beta d}) \end{aligned} \right\} \quad (16-a)$$

while those at $z = -d$ result in

$$\left. \begin{aligned} B_3 e^{-\alpha d} &= A_1 e^{j\beta d} + A_2 e^{-j\beta d} \\ j\alpha B_3 e^{-\alpha d} &= \beta (A_1 e^{j\beta d} - A_2 e^{-j\beta d}) \end{aligned} \right\} \quad (16-b)$$

Elimination of B_1 from the first two equations and B_3 from the second two gives the set

$$\left. \begin{aligned} 0 &= A_1 e^{-j\beta d} \left(1 + \frac{\beta}{j\alpha}\right) + A_2 e^{j\beta d} \left(1 - \frac{\beta}{j\alpha}\right) \\ 0 &= A_1 e^{j\beta d} \left(1 - \frac{\beta}{j\alpha}\right) + A_2 e^{-j\beta d} \left(1 + \frac{\beta}{j\alpha}\right) \end{aligned} \right\}, \quad (17)$$

which has a non-trivial solution for A_1 and A_2 only if the determinant of the coefficients is zero. The vanishing of the determinant yields the surface wave dispersion relation

$$e^{j4\beta d} - \left(\frac{j\alpha + \beta}{j\alpha - \beta}\right)^2 = 0 \quad (18)$$

If expressions (11) and (14) for α and β in terms of k_x, k_y and $k_0 = \omega \sqrt{\epsilon_0 \mu_0}$ are substituted into (18), the dispersion relation is seen to be of the form $D_s(\underline{k}_t, \omega) = 0$.

PROPERTIES OF THE DISPERSION RELATION

As given in (14), β is either real or imaginary for all real k_x and k_y . Let us first verify that no solutions of (18) exist for which β is imaginary. If β is imaginary, i.e., $\beta = \pm j|\beta|$, then (18) becomes

$$e^{\mp 4|\beta|d} = \left(\frac{\alpha \pm |\beta|}{\alpha \mp |\beta|} \right)^2. \quad (19)$$

The left-hand side is less (greater) than unity while the right-hand side is greater (less) than unity. This contradiction verifies the assertion. When β is real, however, both terms in (18) have magnitude unity so that a solution is possible. In order to find the range of frequencies for which (18) has solutions, based on the restriction that β be real, we plot for all $X > 0$ those regions in the $k_x - k_y$ plane where β is real and the region where α is real (see Fig. 2). From Fig. 2 it is seen that the regions where β is real and the region where α is real overlap only when $X > 1$. Hence the possibility that surface waves can propagate exists only for $X > 1$. In passing, observe that (18) remains invariant under the substitution of $-\beta$ for β . Thus it is sufficient to consider only positive values of β . Since the slab configuration has mirror symmetry in the plane $z = 0$, the surface wave fields will correspond to either an open-circuit or a short-circuit bisection of the slab (even and odd solutions in z). The dispersion relation given in (18) can be split into two independent dispersion relations, one giving the open-circuit bisection solutions and the other the short-circuit bisection solutions. These are

$$e^{j2\beta d} = \pm \frac{j\alpha + \beta}{j\alpha - \beta} \quad (20)$$

where the plus and minus signs correspond to short-circuit and open-circuit bisections, respectively. Using the plus sign for the short-circuit bisection case, the dispersion relation may be put in the form

$$\alpha = -\beta \cot \beta d, \quad (21)$$

whereas if the minus sign is used, the dispersion relation for the open-circuit bisection case can be written

$$\alpha = \beta \tan \beta d \quad (22)$$

with α and β as given in (11) and (14).

A graphical method for solving equations (21) and (22) is described below. In order to show that equations (21) and (22) are satisfied for real values of k_x, k_y and $\omega < \omega_p$, i. e., $X > 1$, the plots of (21) and (22) in the $\beta - \alpha$ plane are considered. Since α and β have been taken to be positive, only the first quadrant is of interest.

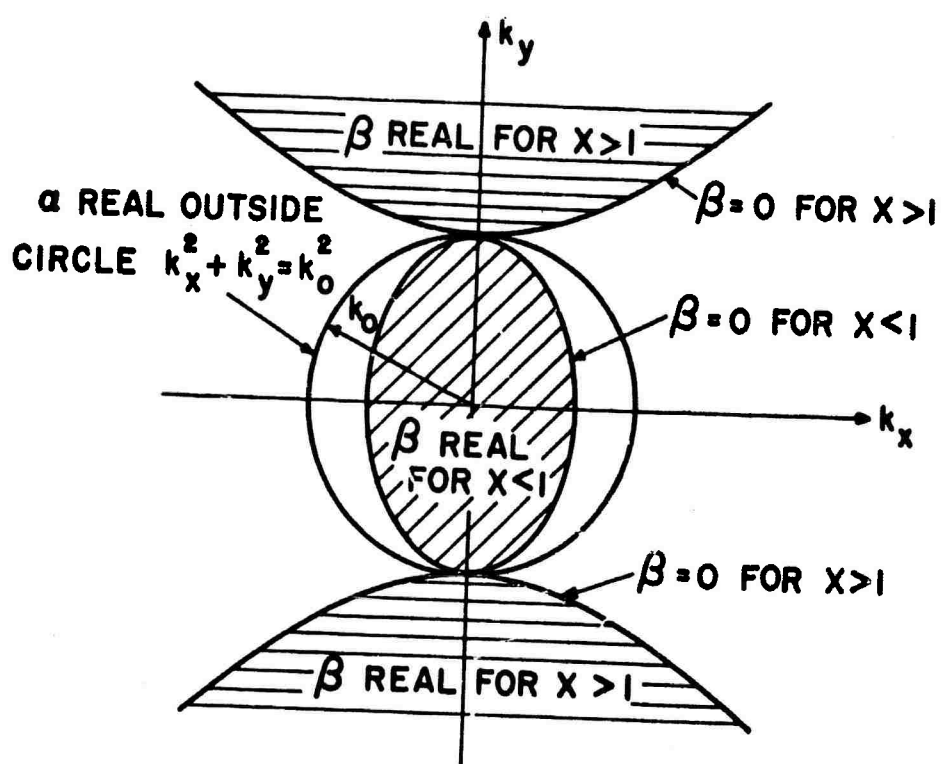


Fig. 2 Regions of Real β and α in the k_x - k_y Plane.

Adding α^2 to β^2 gives $\alpha^2 + \beta^2 = X(k_y^2 - k_0^2)$ when (11) and (14) are used. Because $k_y^2 > k_0^2$ for surface waves, as can be seen from Fig. 2, the plot of this relation in the β - α plane is a circle whose radius is $\sqrt{X(k_y^2 - k_0^2)}$. The intersection of this circle with the plot of (21) or (22) gives α and β from which k_x can be found using

$$k_x = \pm \sqrt{\frac{1}{X} [(X-1)\alpha^2 - \beta^2]} \quad (23)$$

But k_x must be real so that in the first quadrant only those intersections for which $\alpha \geq \frac{1}{\sqrt{X-1}} \beta$ give values of α and β which correspond to an actual surface wave. Since α and β depend only on k_y^2 and k_0^2 and not merely on k_y or k_x , constant ω surface wave dispersion curves will have mirror symmetry about the k_x and k_y axes in the k_x - k_y plane. Thus, knowing the relation between k_x and k_y for $k_x, k_y \geq 0$ is sufficient to determine the entire dispersion curve.

Figure 3 has been sketched to show the method outlined above for finding that k_x which satisfies (21) when k_y and k_0 are given. Each branch of $-\beta \cot \beta d$ depicted in Fig. 3 corresponds to a particular short-circuit bisection surface wave mode. Since there are an infinite number of such branches, there will be an infinite number of short-circuit bisection surface wave modes when $X(k_y^2 - k_0^2) \rightarrow \infty$. For a finite value of $X(k_y^2 - k_0^2)$ only a finite number of surface wave modes can propagate. For values of α and β in the shaded region of Fig. 3, k_x , as found from $k_x = \pm \sqrt{\frac{1}{X} [(X-1)\alpha^2 - \beta^2]}$, is imaginary. Thus it is seen that for fixed k_0 each mode has a minimum value of $k_y^2 > k_0^2$ at which $k_x = 0$ and below which no real solutions for k_x exist. The minimum value of k_y^2 for which a particular surface wave mode can exist is found from the condition that the circle $\alpha^2 + \beta^2 = X(k_y^2 - k_0^2)$, the line $\alpha = \frac{1}{\sqrt{X-1}} \beta$ and that branch of $\alpha = -\beta \cot \beta d$ corresponding to the mode in question all intersect at a common point. As k_y^2 increases from its minimum value, k_y and the corresponding solutions for k_x for each branch of $-\beta \cot \beta d$ trace out the surface wave dispersion curves in the k_x - k_y plane of the short-circuit bisection modes.

In a similar fashion, Fig. 4 depicts the method for finding that k_x which satisfies (22) when k_y and k_0 are given. From this figure and Fig. 3, it is seen that the lowest surface wave mode on the slab, i. e., the one with the smallest value of β , is that open-circuit bisection mode corresponding to the branch of $\beta \tan \beta d$ starting at $\beta = 0$. As in the case of the short-circuit bisection modes, k_x corresponding to values of β and α

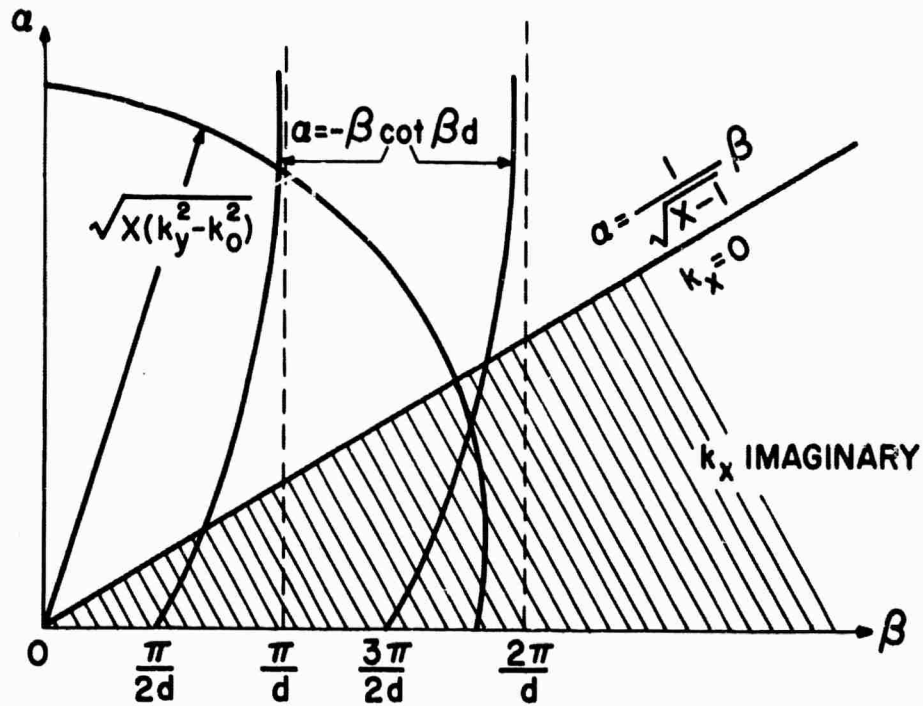


Fig. 3 Construction for Finding Solutions of the Surface Wave Dispersion Relation for the Short-Circuit Bisection Case.

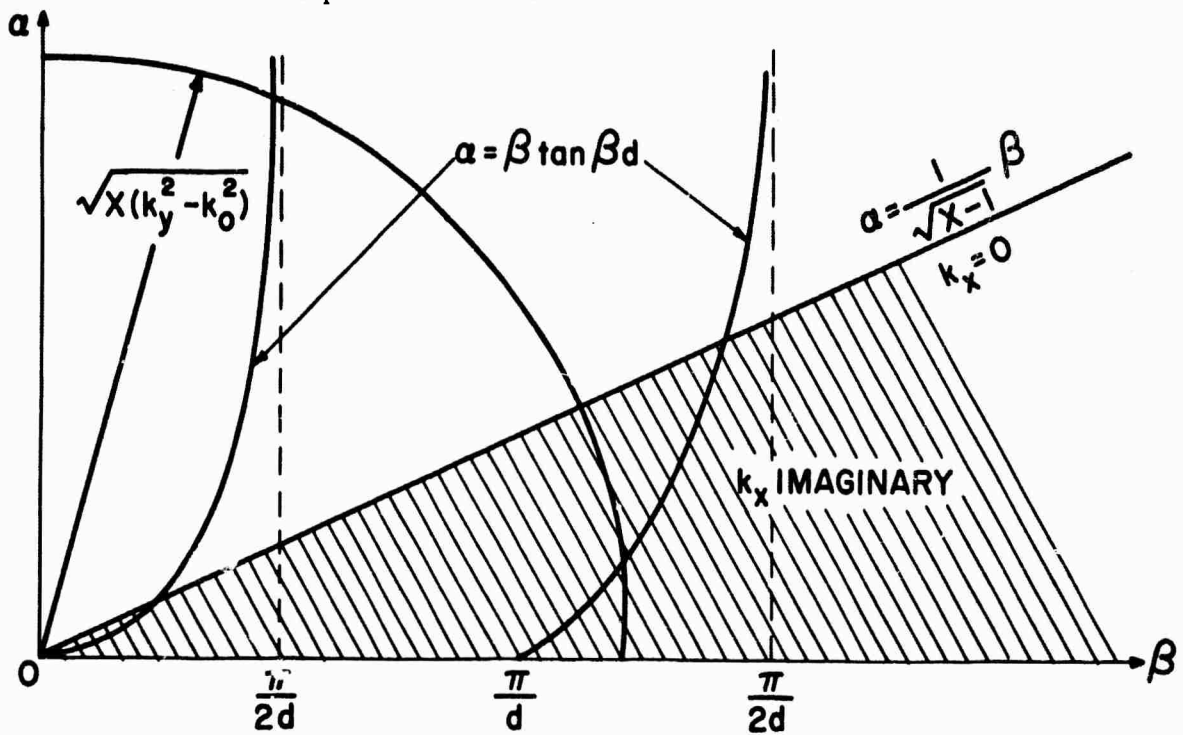


Fig. 4 Construction for Finding Solutions of the Surface Wave Dispersion Relation for the Open-Circuit Bisection Case.

in the shaded region of Fig. 4 is imaginary. Thus for each of the higher open-circuit bisection modes there will be a minimum value of $k_y^2 > k_o^2$ at which $k_x = 0$ and below which no real solution for k_x exists. For the lowest open-circuit bisection mode $[\frac{d}{d\beta}(\beta \tan \beta d)]_{\beta=0} = 0$ so that a part of the branch of $\beta \tan \beta d$ starting at $\beta=0$ lies in the shaded region of Fig. 4. Hence there will also be a minimum value of $k_y^2 > k_o^2$ for the lowest surface wave mode below which no real solution for k_x exists. As in the short-circuit bisection case, when k_y^2 increases from its minimum value for a particular mode and for a fixed k_o , k_y and the corresponding value of k_x trace out the dispersion curve of that open-circuit bisection mode.

In what follows, the basic properties of the surface wave dispersion curves will be derived. For any one mode, these properties lead to the form of the dispersion curves shown in Fig. 5, which has been drawn for two different frequencies $\omega_2 > \omega_1$. In order to find the shape of the dispersion curves of any one mode and for fixed ω , we consider the corresponding branch of $-\beta \cot \beta d$ in Fig. 3 or of $\beta \tan \beta d$ in Fig. 4. As pointed out previously, the dispersion curves are symmetric about the k_x and k_y axes so that we need find only that portion of the curves in the first quadrant of Fig. 5. Also, as was previously discussed, in the first quadrant of Fig. 5, k_y takes on its minimum value, which is greater than k_o , at $k_x = 0$, i. e., where the dispersion curve crosses the k_y axis. It will first be shown that in the first quadrant, k_x is a single-valued, monotonically increasing function of k_y . These two facts indicate that the inverse function, $k_y = k_y(k_x)$, is single-valued and monotonically increasing in the first quadrant as is depicted in Fig. 5. Other fundamental properties of that portion of the dispersion curve in the first quadrant of Fig. 5 that will be established are: 1) $dk_y/dk_x = 0$ at $k_x = 0$; 2) asymptotically as $k_y \rightarrow \infty$, $k_x \sim k_y/\sqrt{X-1}$ and the dispersion curve everywhere lies above the asymptote $k_y = k_x/\sqrt{X-1}$; 3) the value of k_y at $k_x = 0$, as well as the slope of the asymptote, increase with ω . One question that has not yet been answered analytically is whether the surface wave dispersion curves have inflection points.

To see that in the first quadrant of Fig. 5, k_x is a single-valued function of k_y , observe that for $\beta > 0, \alpha > 0$ each branch of $-\beta \cot \beta d$ in Fig. 3 and each branch of $\beta \tan \beta d$ in Fig. 4 intersects the circle $\alpha^2 + \beta^2 = X(k_y^2 - k_o^2)$ only once. Thus for a given ω_p and for each value of k_y and ω there will be only one set of values (β, α) for each mode and hence from (23) only one value of $k_x > 0$ for each mode. Therefore, in the first quadrant of Fig. 5, k_x is a single-valued function of k_y . That k_x is a monotonically increasing function of k_y can be inferred from the sign of dk_x/dk_y . Since k_x and k_y satisfy the

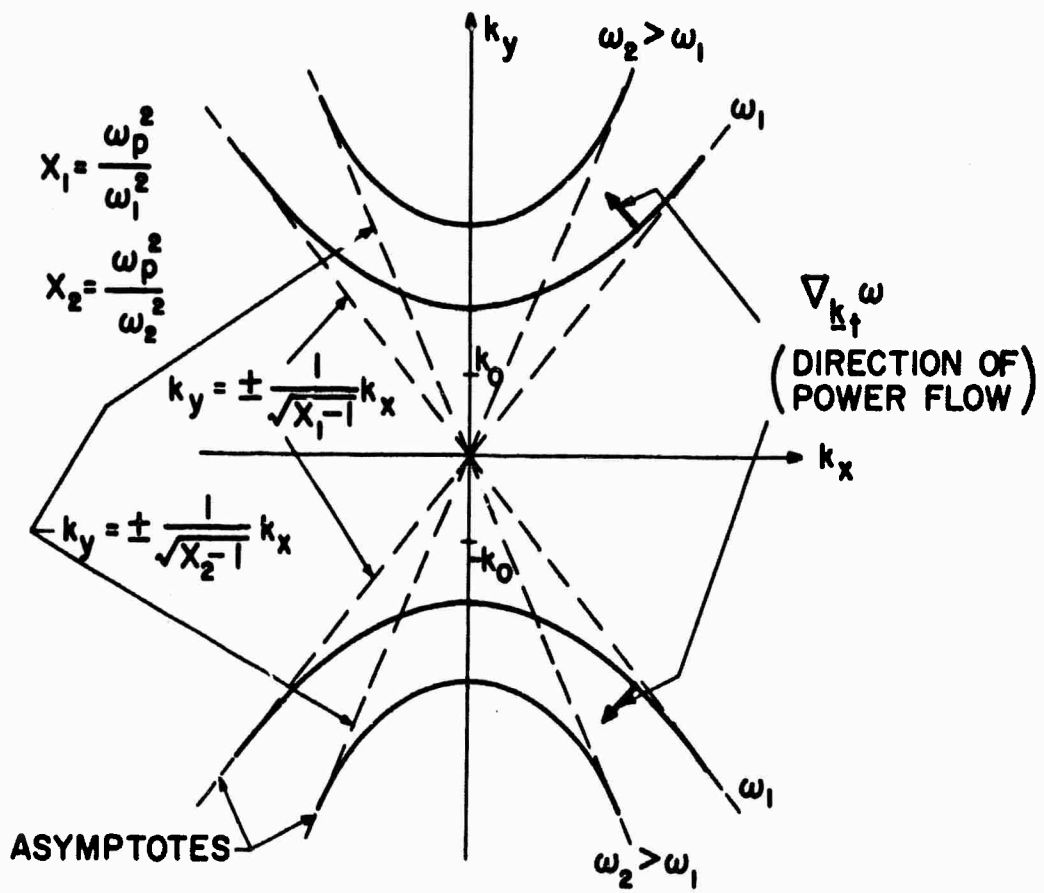


Fig. 5 Dispersion Curves for a Typical Surface Wave Mode With ω as a Parameter.

surface wave dispersion relation $D_s(k_x, \omega) = 0$, dk_x/dk_y for fixed ω is given by $dk_x/dk_y = - \frac{\partial D_s / \partial k_y}{\partial D_s / \partial k_x}$. Using D_s as given in the left-hand side of (18), with α and β defined in (11) and (14), it is found that

$$\frac{dk_x}{dk_y} = \frac{k_y}{k_x} - \frac{\alpha d(X-1) + k_x^2 / (k_y^2 - k_o^2)}{\alpha d + 1} \quad (24)$$

From (24) we see that in the first quadrant of Fig. 5, $dk_x/dk_y > 0$ and hence, $k_x(k_y)$ is a monotonically increasing function. Furthermore, (24) shows that $dk_y/dk_x = 0$ at $k_x = 0$ as is depicted in Fig. 5.

As $k_y \rightarrow \infty$, the value of β at the intersection of the circle $\alpha^2 + \beta^2 = X(k_y^2 - k_o^2)$ and any one branch of $-\beta \cot \beta d$ in Fig. 3 or any one branch of $\beta \tan \beta d$ in Fig. 4 approaches a constant. Thus, since k_o has been assumed constant, $\alpha^2 \sim Xk_y^2$ as $k_y \rightarrow \infty$ and hence, from (23), k_x in the first quadrant of Fig. 5 is asymptotically given by $k_x \sim k_y \sqrt{X-1}$ or conversely $k_y \sim k_x / \sqrt{X-1}$. That the dispersion curve lies above the asymptote line $k_y = k_x / \sqrt{X-1}$, as shown in the first quadrant of Fig. 5, can be deduced from the definition of β given in (14). Since β is real for the surface waves and $X > 1$, $(X-1)k_y^2 - k_x^2 = \beta^2 + k_o^2(X-1) > 0$ and therefore in the first quadrant $k_y > k_x / \sqrt{X-1}$, which proves that the dispersion curve lies above the asymptote line. When ω increases but remains below ω_p , X decreases to unity and hence the slope of the asymptote, $1/\sqrt{X-1}$, increases as is depicted in Fig. 5. Furthermore, as ω increases the slope of the line $\alpha = \beta / \sqrt{X-1}$ in Fig. 3 and Fig. 4 increases. Hence the values of β and α at $k_x = 0$, as determined from the intersection of the line $\alpha = \beta / \sqrt{X-1}$ with any branch of $-\beta \cot \beta d$ in Fig. 3 or of $\beta \tan \beta d$ in Fig. 4, must increase. Because k_o increases with ω and X decreases, the quantity $\frac{1}{X}(\alpha^2 + \beta^2) + k_o^2 = k_y^2$ must increase and thus the magnitude of k_y at $k_x = 0$ increases with ω . The above-described variation with ω of k_y at $k_x = 0$ is depicted in Fig. 5.

Thus the fundamental properties previously stated for the surface wave dispersion curves of any one mode are seen to hold. These properties indicate that the dispersion curves will have the form depicted in Fig. 5, with the possible exception of inflection points, for two different frequencies. From Fig. 3 and Fig. 4 it can also be seen that surface waves exist for all ω in the range $0 < \omega < \omega_p$. Lastly, since in the first quadrant of Fig. 5, $\frac{dk_y}{dk_x} \geq 0$, which follows from (24), and since the dispersion curve for $\omega = \omega_2$ lies

above that for $\omega = \omega_1 < \omega_2$, the x component of $\nabla_{\underline{k}} \omega$ must everywhere be negative. That the dispersion curve for $\omega = \omega_2$ lies above that for $\omega = \omega_1$ follows from the fact that at $k_x = 0$ the $\omega = \omega_1$ curve lies above the $\omega = \omega_2$ curve and the two curves never cross since $\nabla_{\underline{k}_t} \omega$, which is given in (42), is never infinite. The observation that $\underline{x}_0 \cdot \nabla_{\underline{k}_t} \omega > 0$ is confirmed by the analytic expression for $\nabla_{\underline{k}_t} \omega$ given in (42) and indicates that the surface waves are of the backward wave type with respect to the x direction.

GROUP VELOCITY AND ENERGY TRANSPORT VELOCITY

Having established the basic properties of the dispersion relation of the surface waves on a uniaxial plasma slab, the equality of group velocity and energy transport velocity for these surface waves will be verified by direct calculation. This relation is given in Reference (1) as

$$\nabla_{\underline{k}_t} \omega = \frac{\int_{-\infty}^{\infty} \underline{s} dz}{\int_{-\infty}^{\infty} w dz} \quad (25)$$

where \underline{s} represents the real part of the complex Poynting vector $\underline{E} \times \underline{H}^*$ and w the time average stored energy density. To this end, the relative field amplitudes are first calculated. Since one of the coefficients A_1, A_2, B_1 and B_3 is arbitrary, for simplicity let

$$A_1 = -A_0(\beta - j\alpha)e^{j\beta d} \quad (26)$$

where A_0 is arbitrary. Then from (17) it is found that

$$A_2 = -A_0(\beta + j\alpha)e^{-j\beta d} \quad (27)$$

while from (16-a)

$$B_1 = -2\beta A_0 e^{\alpha d} \quad (28)$$

Using the dispersion relation in the form given in (18), which is valid for both open-circuit and short-circuit bisection modes, it follows that

$$B_3 = -2\beta A_0 \frac{\beta + j\alpha}{\beta - j\alpha} e^{-j2\beta d} e^{\alpha d} . \quad (29)$$

With these expressions in equations (12), (13) and (15) for the fields in the three regions, \underline{s} in Region 1 is found to be

$$\underline{s} = 4|A_0|^2 \beta^2 \omega \epsilon_0 e^{-2\alpha(z-d)} [\underline{x}_0 k_x (k_o^2 - k_y^2) + \underline{y}_0 k_y (\alpha^2 + k_x^2)] \quad (30)$$

while in Region 3 it is

$$\underline{s} = 4|A_0|^2 \beta^2 \omega \epsilon_0 e^{2\alpha(z+d)} [\underline{x}_0 k_x (k_o^2 - k_y^2) + \underline{y}_0 k_y (\alpha^2 + k_x^2)] \quad (31)$$

and finally in Region 2 it is

$$\begin{aligned} \underline{s} = & |A_0|^2 \omega \epsilon_0 (\alpha^2 + \beta^2) \left\{ 2 [\underline{x}_0 k_x (k_o^2 - k_y^2) + \underline{y}_0 k_y (\beta^2 + k_x^2)] + \right. \\ & \left. + \left[\frac{\beta + j\alpha}{\beta - j\alpha} e^{j2\beta(z-d)} + \frac{\beta - j\alpha}{\beta + j\alpha} e^{-j2\beta(z-d)} \right] \cdot [\underline{x}_0 k_x (k_o^2 - k_y^2) + \underline{y}_0 k_y (k_y^2 - \beta^2)] \right\} . \end{aligned} \quad (32)$$

The quantity $\underline{S} = \int_{-\infty}^{\infty} \underline{s} dz$ is now calculated to be

$$\begin{aligned} \underline{S} = & 4|A_0|^2 \omega \epsilon_0 (\alpha^2 + \beta^2) \left\{ -\underline{x}_0 k_x (k_y^2 - k_o^2) \left[\frac{1}{\alpha} + d \right] \right. \\ & \left. + \underline{y}_0 k_y \left[\frac{1}{\alpha} k_x^2 + d(X-1)(k_y^2 - k_o^2) \right] \right\} . \end{aligned} \quad (33)$$

In order to determine the stored energy, observe that in the plasma slab

$$\left[\frac{\partial \omega \epsilon}{\partial \omega} \right] = \epsilon_0 \left[\frac{\partial \omega \epsilon'}{\partial \omega} \right] = \epsilon_0 \begin{bmatrix} 1 & 0 & 0 \\ 0 & 1+X & 0 \\ 0 & 0 & 1 \end{bmatrix} . \quad (34)$$

Thus in Region 2, the time averaged stored energy density, which is given by^(7, 8),

$$w = \frac{1}{2} \left[\underline{E}^* \cdot \frac{\partial \omega \epsilon}{\partial \omega} \cdot \underline{E} + \mu_0 |\underline{H}|^2 \right] , \quad (35)$$

is found to be

$$w = \frac{1}{2} |A_o|^2 \epsilon_o (\alpha^2 + \beta^2) \left\{ 4(k_y^2 - k_o^2)(Xk_y^2 - k_o^2) - \left[\frac{\beta + j\alpha}{\beta - j\alpha} e^{j2\beta(z-d)} + \frac{\beta - j\alpha}{\beta + j\alpha} e^{-j2\beta(z-d)} \right] \cdot [(\beta^2 - k_x^2)(k_o^2 + k_y^2) - (1+X)(k_y^2 - k_o^2)] \right\} \quad (36)$$

Outside the slab, the time averaged stored energy density has the form

$$w = \frac{1}{2} [\epsilon_o |\underline{E}|^2 + \mu_o |\underline{H}|^2] \quad (37)$$

so that in Region 1

$$w = 2 |A_o|^2 \epsilon_o \beta^2 [(k_o^2 + k_y^2)(k_x^2 + \alpha^2) + (k_y^2 - k_o^2)^2] e^{-2\alpha(z-d)} \quad (38)$$

while in Region 3

$$w = 2 |A_o|^2 \epsilon_o \beta^2 [(k_o^2 + k_y^2)(k_x^2 + \alpha^2) + (k_y^2 - k_o^2)^2] e^{2\alpha(z+d)} \quad (39)$$

Calculating $W = \int_{-\infty}^{\infty} w dz$, it is found that

$$W = 4 |A_o|^2 \epsilon_o (\alpha^2 + \beta^2) \left\{ d(k_y^2 - k_o^2)(Xk_y^2 - k_o^2) + \frac{1}{\alpha} [k_x^2 k_y^2 + (k_y^2 - k_o^2)^2] \right\} \quad (40)$$

In deriving the above power and energy formulas, extensive use has been made of the dispersion relation given in (18) and the formulas (11) and (14) for α and β . Using the above expressions for \underline{S} and W , the energy transport velocity is seen to be

$$\frac{\underline{S}}{W} = w \frac{-\underline{x}_o k_x (k_y^2 - k_o^2)(\frac{1}{\alpha} + d) + \underline{y}_o k_y [\frac{1}{\alpha} k_x^2 + d(X-1)(k_y^2 - k_o^2)]}{d(k_y^2 - k_o^2)(Xk_y^2 - k_o^2) + \frac{1}{\alpha} [k_x^2 k_y^2 + (k_y^2 - k_o^2)^2]} \quad (41)$$

In order to compute the group velocity $\nabla_{\underline{k}_t} w$, the formula $\nabla_{\underline{k}_t} w = -\nabla_{\underline{k}_t} D_s / \frac{\partial D_s}{\partial w}$ from implicit function theory will be used where the function $D_s(\underline{k}_t, w)$ is the left-hand

side of (18). It is found that

$$\nabla_{\underline{k}} \omega = \omega \frac{\underline{x}_0 k_x \left(\frac{1}{\alpha} + d \right) + \underline{y}_0 k_y \left[d(X-1) + \frac{k_x^2 X}{\alpha(\alpha^2 + \beta^2)} \right]}{d(Xk_y^2 - k_o^2) + \frac{1}{\alpha}(k_y^2 - k_o^2) + \frac{k_x^2 k_y^2}{\alpha(k_y^2 - k_o^2)}} \quad (42)$$

If both the numerator and denominator of the above expression are multiplied by $(k_y^2 - k_o^2)$ and it is recognized that $X(k_y^2 - k_o^2) = \alpha^2 + \beta^2$, $\nabla_{\underline{k}} \omega$ will be seen to be identical with \underline{S}/W , as predicted in Reference 1.

The example worked out above also illustrates the fact that, in general, the direction of \underline{s} as well as its magnitude can vary with z . This can be seen from equation (32) for \underline{s} in Region 2 if it is recognized that the vectors $[\underline{x}_0 k_x (k_o^2 - k_y^2) + \underline{y}_0 k_y (\beta^2 + k_x^2)]$ and $[\underline{x}_0 k_x (k_o^2 - k_y^2) + \underline{y}_0 k_y (k_x^2 - \beta^2)]$ are parallel only for $k_x = 0$. Since the coefficient of the first vector is independent of z while the coefficient of the second vector depends on z , the direction of the vector sum, which gives \underline{s} , will depend on z for all surface waves for which $k_x \neq 0$.

APPENDIX

The purpose of this Appendix is to investigate the possible contribution to a surface wave field from the plane wave fields in the plasma that are associated with the solutions $\kappa = \pm \sqrt{k_o^2 - k_t^2}$ of the plasma plane wave dispersion relation. The vector character of these plasma plane waves is that of H-type modes and has the form

$$\left. \begin{aligned} \underline{e}' &= C[\underline{x}_o \kappa - \underline{z}_o k_x] \\ \underline{h}' &= \frac{C}{\omega \mu_o} [-\underline{x}_o k_y k_x + \underline{y}_o (k_o^2 - k_y^2) - \underline{z}_o \kappa k_y] \end{aligned} \right\} \quad (43)$$

with C an arbitrary constant. The vector character of those plane waves in the air regions that have the H-type mode form, and will thus allow a simple application of the continuity conditions at $z = \pm d$, is

$$\left. \begin{aligned} \underline{e}'_a &= D[\underline{x}_o \kappa_a - \underline{z}_o k_x] \\ \underline{h}'_a &= \frac{D}{\omega \mu_o} [-\underline{x}_o k_y k_x + \underline{y}_o (k_o^2 - k_y^2) - \underline{z}_o \kappa_a k_y] \end{aligned} \right\} \quad (44)$$

with $\kappa_a = \pm j\alpha$ and α as defined in (11). Note that $\kappa = \pm j\alpha$ also.

In Region 1, κ_a must be taken as $-j\alpha$ to ensure that \underline{E} and \underline{H} are zero at $z = \infty$. Similarly, in Region 3, κ_a must be taken as $j\alpha$. Denoting the amplitudes in Regions 1 and 3 as D_1 and D_3 , respectively, and letting C_1 and C_2 be the amplitudes of the plasma plane waves corresponding to $\kappa = -j\alpha$ and $\kappa = j\alpha$, respectively, the continuity conditions at $z = d$ result in the equations

$$\left. \begin{aligned} -D_1 e^{-\alpha d} &= -C_1 e^{-\alpha d} + C_2 e^{\alpha d} \\ D_1 e^{-\alpha d} &= C_1 e^{-\alpha d} + C_2 e^{\alpha d} \end{aligned} \right\} \quad (45)$$

when the fields in Region 2 are assumed to be the sum of the two H-type plane waves. The continuity conditions at $z = -d$ can be written as

$$\left. \begin{aligned} D_3 e^{-\alpha d} &= -C_1 e^{\alpha d} + C_2 e^{-\alpha d} \\ D_3 e^{-\alpha d} &= C_1 e^{\alpha d} + C_2 e^{-\alpha d} \end{aligned} \right\} \quad (46)$$

These equations have only the trivial solutions $C_1 = C_2 = D_1 = D_3 = 0$ and hence no surface wave can exist whose fields in the plasma are a sum of the two H-type plasma plane waves, which propagate as $\kappa = \pm j\alpha$.

The physical reason why no surface wave exists that contains the above-mentioned plane waves is that the waves of this polarization do not "see" the plasma, since the infinite D. C. magnetic field along y prevents the electrons from moving in response to an R. F. electric field that, as in this case, is purely transverse to y . In effect, for waves of this polarization, no slab on which to have surface waves is present.

REFERENCES

1. H. L. Bertoni and A. Hessel, "Group Velocity and Power Flow Relations for Surface Waves in Plane-Stratified Anisotropic Media", Microwave Research Institute, Polytechnic Institute of Brooklyn, Report PIBMRI 1293-65 (1965).
2. J. R. Wait, "Propagation of Electromagnetic Waves Along a Thin Plasma Sheet", Canadian Journal of Physics 38 (1960), pp. 1586-1594.
3. G. Meltz and R. A. Shore, "Leaky Waves Supported by Uniaxial Plasma Layers", IEEE Trans. AP-13 (1965), pp. 94-105.
4. F. M. Labianca, "The Electromagnetic Fields of Certain Uniaxially Anisotropic Dielectric Slabs", Microwave Research Institute, Polytechnic Institute of Brooklyn, Report PIBMRI 1150-63 (1963).
5. H. Hodara and G. I. Cohn, "Wave Propagation in Magneto-Plasma Slabs", IRE Trans. AP-10 (1962), pp. 452-459.
6. S. R. Seshadri and W. F. Pickard, "Surface Waves on an Anisotropic Plasma Sheath", IEEE Trans. MTT-12 (1964), pp. 529-541.
7. L. D. Landau and E. M. Lifshitz, "Electrodynamics of Continuous Media", Pergamon Press, New York (1960), pp. 253-256, 314.
8. T. H. Stix, "The Theory of Plasma Waves", McGraw-Hill Book Company, New York (1962), pp. 45-48.

Advanced Research Projects
Agency
Attn: Dr. B.S. Fisher
The Pentagon
Washington, D.C. 20301

Advanced Research Projects
Agency
Attn: Maj. R.M. Dowe, Jr.
The Pentagon
Washington, D.C. 20301

Advanced Research Projects
Agency
Attn: Mr. C.E. McLain
The Pentagon
Washington, D.C. 20301

Advanced Research Projects
Agency
Attn: Mr. F.A. Koether
The Pentagon
Washington, D.C. 20301

Advanced Research Projects
Agency
Attn: Dr. P.L. Auer
The Pentagon
Washington, D.C. 20301

Advanced Research Projects
Agency
Attn: Dr. R. Zirkind
The Pentagon
Washington, D.C. 20301

Advanced Research Projects
Agency
Attn: Major H. Dickinson
The Pentagon
Washington, D.C. 20301

Aerojet-General Corporation
Attn: Technical Library
P.O. Box 296
Azusa, California

Aeronutronic Division
Philco Corporation
Attn: Dr. H. Shenfield
Ford Road
Newport Beach, California

Aerospace Corporation
Attn: Manager, Penetration Aids
2400 E. El Segundo Blvd.
El Segundo, California

Aerospace Corporation
Norton Air Force Base
Attn: Mr. William Barry
San Bernardino, California

Aerospace Corporation
Norton Air Force Base
Attn: Dr. H. Meyers
San Bernardino, California

Air Force Cambridge Research
Laboratory
Attn: Scientific Library
CRREL, Stop 29
L.G. Hanscom Field
Bedford, Mass.

Air Force Cambridge Research
Laboratory
Attn: Dr. Norman W. Rosenberg
L.G. Hanscom Field
Bedford, Mass.

Air Force Cambridge Research
Laboratory
Attn: Dr. K. Champion
L.G. Hanscom Field
Bedford, Mass.

Air Force Cambridge Research
Laboratory
Attn: Dr. A.T. Stair (CROR)
L.G. Hanscom Field
Bedford, Mass.

Air Force Office of Scientific
Research
Attn: Dr. M.C. Harrington
Washington, D.C.

Air Force Office of Scientific
Research
Attn: Dr. D.L. Wennersten
Washington, D.C.

Army Missile Command
Attn: AMCPM-ZER-R
Redstone Arsenal
Huntsville, Alabama

Army Missile Command
Attn: AMSMI-RB
Redstone Arsenal
Huntsville, Alabama

Army Missile Command
Attn: AMSMI-RNM
Redstone Arsenal
Huntsville, Alabama

Army Research Office
Attn: Dr. Hermann Robl
Box C.M. Duke Station
Durham, N.C. 27706

Army Technical Intelligence
Agency
Attn: ORDLI
Arlington Hall Station
Arlington, Virginia

Air Force Weapons Laboratory
Attn: Capt. David Sparks
Kirtland Air Force Base
Albuquerque, N.M.

Air Force Weapons Laboratory
Attn: Capt. William Whittaker
Kirtland Air Force Base
Albuquerque, N.M.

Applied Physics Laboratory
Johns Hopkins University
Attn: Dr. Felix Falls
Howard County, Maryland

Arecibo Ionospheric Observa-
tory
Attn: Dr. W.E. Gordon, Dir.
Box 995
Arecibo, Puerto Rico

Australian Embassy
Attn: D. Barnsley, Defense
R. and E. Representative
2001 Connecticut Ave., NW
Washington, D.C.

Avco-Everett Research Lab.
Attn: Technical Library
2385 Revere Beach Pkwy.
Everett 49, Mass.

Avco-Everett Research Lab.
Attn: Mr. P. Rose
2385 Revere Beach Pkwy.
Everett 49, Mass.

Avco-Research and Advanced
Development Div.
Attn: Mr. Harold Debolt
201 Lowell Street
Wilmington, Mass.

Avco-Research and Advanced
Development Div.
Attn: Dr. A. Pallone
201 Lowell Street
Wilmington, Mass.

Ballistics Research Laboratory
Attn: Dr. C.H. Murphy
Aberdeen Proving Ground, Md.

Battelle Memorial Institute
ATTN: Battelle-DEFENDER
505 King Avenue
Columbus 1, Ohio

Cornell University
Nuclear Studies Laboratory
Attn: Dr. Edwin E. Salpeter
Ithaca, N. Y.

General Dynamics Corporation
Convair Division
Attn: Dr. Klaus G. Sulzmann
P.O. Box 166
San Diego, Calif.

Bell Telephone Laboratories
Attn: Dr. C. W. Hoover
Whippany, N. J.

Defense Atomic Support Agency
Attn: Dr. T. Taylor, Deputy
Director, Scientific
The Pentagon 1 B 697
Washington, D. C.

General Electric Co., MSVD
Document Library
Reentry Physics Library Unit
Attn: Mgr. -MSVD Library 3446
3198 Chestnut Street
Philadelphia, Pa.

Bendix Systems Division
Flight Sciences Department
Ann Arbor, Michigan

Defense Atomic Support Agency
Attn: Dr. C. Blank
The Pentagon 1 B 697
Washington, D. C.

General Electric Research Lab.
Attn: Dr. George C. Baldwin
(General Engineering Lab)
Schenectady, New York

British Joint Mission
British Embassy
Attn: Mr. A. N. Mosses, Defense
Research Staff
3100 Massachusetts Ave., NW
Washington, D. C.
Brown University
Department of Chemistry
Attn: Dr. John Ross
Providence 12, Rhode Island

Defense Documentation Center
Cameron Station
Alexandria, Virginia 22314

20 copies

Defense Research Corporation
Attn: Dr. Bernard A. Lippman
P.O. Box 3587
Santa Barbara, California

General Electric Space Sciences
Laboratory
Attn: Dr. T. Reithoff
Valley Forge Space Tech. Ctr.
P.O. Box 8555
Valley Forge, Pennsylvania

General Electric Tempo
Attn: Dr. R. Hendrick
Santa Barbara, California

Bureau of Naval Weapons
Special Projects Office
Attn: Commander Julian, SP-25
Munitions Bldg.
Washington, D. C.

Electro-Optical Systems, Inc.
Attn: Mr. Denison
300 N. Halstead Street
Pasadena, California

General Motors
Defense Research Laboratory
Attn: Mr. C. M. Shaar
Box T
Santa Barbara, California

Canadian Armament Research
and Development Establish.
Attn: U.S. Army Liaison Officer
P.O. Box 1427
Quebec, P.Q., Canada

General Applied Science Labs.
Attn: Library
Merrick and Stewart Avenues
Westbury, L.I., N. Y.

Geophysics Corp. of America
Burlington Road
Bedford, Mass.

Air Force Cambridge Research
Laboratory
CRUB
Attn: Dr. K. Champion
Bedford, Mass.

General Applied Science Labs.
Attn: Mr. Walter Daskin
Merrick and Stewart Avenues
Westbury, L.I., N. Y.

Harvard University
Chemistry Department
Attn: Dr. Dudley R. Hershbach
Cambridge, Mass.

Central Intelligence Agency
Attn: OCR Standard Distribution
2430 E St., NW
Washington, D. C.

General Atomic
Attn: Dr. Ronald Stebbings
P.O. Box 608
San Diego 12, California

Headquarters BSD (AFSC)
Air Force Unit Post Office
Attn: BSRVD
Los Angeles 45, California

Chief of Naval Operations
Attn: OP-07TIO
Washington, D. C.

General Dynamics Corporation
Convair Division
Attn: Mr. K. G. Blair, Chief
Librarian
P.O. Box 166
San Diego, California

Heliodyne Corporation
Attn: Dr. Saul Feldman
2365 Westwood Blvd.
Los Angeles, Calif.

Cornell Aeronautical Lab., Inc.
Attn: Mr. A. Hertzberg
P.O. Box 235
Buffalo 21, N. Y.

General Dynamics Corporation
Convair Division
Attn: Dr. Roy H. Neynaber
P.O. Box 166
San Diego, Calif.

Illinois Institute of Technology
Research Institute
Attn: Dr. Carsten Haaland
10 West 35th Street
Chicago, Ill.

Institute for Defense Analyses
Attn: Dr. W. Culver
400 Army-Navy Drive
Arlington, Virginia

Lockheed Missiles and Space Co.
Attn: Dr. Leon Fisher
3251 Hanover Street
Palo Alto, California

National Bureau of Standards
Attn: Dr. Kurt E. Shuler
Washington, D. C.

Institute for Defense Analysis
Attn: Dr. A. Hochstim
400 Army-Navy Drive
Arlington, Virginia
2 copies

Monsanto Research Corporation
Dayton Laboratory
Attn: Dr. J. W. Butler
1515 Nicholas Road
P. O. Box 8, Station B
Dayton, Ohio
Naval Ordnance Laboratory
Attn: Librarian
White Oak
Silver Spring, Maryland

National Bureau of Standards
Attn: Dr. E. L. Brady,
National Standard Reference
Data Center
Washington, D. C.

Institute for Defense Analyses
Attn: Dr. D. Katcher,
JASON Library
400 Army-Navy Drive
Arlington, Virginia

New York University
Attn: Dr. Benjamin Bederson
Physics Department
University Heights
New York 53, N. Y.

Institute for Defense Analyses
Attn: Dr. J. Menkes
400 Army-Navy Drive
Arlington, Virginia

Naval Research Laboratory
Attn: Dr. Alan Kolb, Code 7470
Washington 25, D. C.

New York University
Attn: Dr. Sidney Borowitz
Physics Department
University Heights
New York 53, N. Y.

Institute for Defense Analyses
Attn: Dr. H. Wolfhard
400 Army-Navy Drive
Arlington, Virginia

Naval Research Laboratory
Attn: Code 2027
Washington 25, D. C.

Oak Ridge National Laboratory
Attn: Dr. S. Datz
P. O. Box X
Oak Ridge, Tenn.

Institute for Molecular Physics
Attn: Dr. Edward A. Mason
University of Maryland
College Park, Maryland

National Aeronautics and Space
Administration
Attn: Applied Materials and
Physics Div.
Langley Research Center
Hampton, Virginia

Office of Naval Research
Department of the Navy
Attn: Dr. S. G. Reed,
Jr. Science Director
Washington, D. C.

Joint Institute for Lab Astrophysics
N. B. S., University of Colorado
Attn: Dr. Lewis Branscomb
1511 University Avenue
Boulder, Colorado

National Aeronautics and Space
Administration
Attn: Mail Stop 213
Langley Research Center
Hampton, Virginia

Office of Naval Research
Department of the Navy
Attn: Dr. J. H. Shenk
Materials Science Div.
Washington, D. C.

Jet Propulsion Laboratory
Attn: Library
4800 Oak Grove Drive
Pasadena, California

National Aeronautics and Space
Administration
Attn: Dr. Robert F. Fellows,
Code SL
Langley Research Center
Hampton, Virginia

Office of Naval Research
Department of the Navy
Attn: Dr. W. E. Wright,
Physical Sciences Div.
Washington, D. C.

Kansas State University
Attn: Prof. Basil Curnutte
Physics Department
Manhattan, Kansas

National Aeronautics and Space
Administration
Attn: Dr. Alfred Gessow,
Code RRP
Washington, D. C.

Office of Naval Research
Department of the Navy
Attn: Dr. F. T. Byrne
Physics Section
Washington, D. C.

Lincoln Laboratory, M. I. T.
Attn: Dr. M. Balser
P. O. Box 73
Lexington, Mass.

National Bureau of Standards
Attn: Dr. Karl G. Kessler, Chief
Atomic Physics Div.
Washington, D. C.

Polytechnic Institute of Brooklyn
Attn: Mr. Jerome Fox
Research Office
333 Jay Street
Brooklyn, New York

Lockheed Missiles and Space Co.
Attn: Dr. R. Myerott
3251 Hanover Street
Palo Alto, California

National Bureau of Standards
Attn: Dr. M. B. Wallenstein,
Chief, Physical Chem. Div.
Washington, D. C.

Queen's University of Belfast
Attn: Professor D. R. Bates
Department of Applied Math.
Belfast 7, Northern Ireland, UK

Radio Corp. of America
Missile and Surface Radar Div.
Moorestown, N. J.

RCA-Victor Co., Ltd.
Research Laboratories
Attn: Dr. A. I. Carswell
1001 Lenoir Street
Montreal 30, Canada

The Rand Corporation
Attn: Library
1700 Main Street
Santa Monica, California

The Rand Corporation
Attn: Dr. R. Hundley
1700 Main Street
Santa Monica, California

The Rand Corporation
Attn: Dr. Forrest R. Gilmore
1700 Main Street
Santa Monica, California

The Rand Corporation
Attn: Dr. Robert E. LeLevier
1700 Main Street
Santa Monica, California

Rocketdyne Division
North American Aviation, Inc.
Attn: Dr. S. A. Golden
Physics Group
6633 Canoga Avenue
Canoga Park, Calif. 91304
Sperry Rand Research Center
Attn: Dr. Philip M. Stone
North Road (Route 117)
Sudbury, Mass.

Space Technology Laboratories
Attn: Dr. L. Hromas
1 Space Park
Redondo Beach, California

Stanford Research Institute
Attn: Dr. C. J. Cook, Director
Chemical Physics Div.
333 Ravenswood Avenue
Menlo Park, California

Stanford Research Institute
Attn: Dr. Carson Flammer, Mgr.
Mathematical Division
333 Ravenswood Avenue
Menlo Park, California

United Aircraft Corporation
Research Laboratories
Attn: Dr. Russell G. Meyerand
East Hartford 8, Conn.

University of Alabama
Attn: Dr. Erich Rodgers
Physics Department
P. O. Box 1921
University, Alabama

University of California
Attn: Prof. Kenneth Watson
Physics Department
Berkeley, California

University of California
Lawrence Radiation Laboratory
Attn: Dr. Marvin Mittleman
Box 808
Livermore, California

University of California
Attn: Dr. Herbert P. Broida
Department of Physics
Santa Barbara, Calif.

Dr. Keith A. Brueckner
University of California
San Diego
P. O. Box 109
La Jolla, Calif. 92038

University of Chicago
Attn: Dr. John Light,
Chemistry Department
Chicago, Ill.

University of Chicago
Attn: Prof. C. C. J. Roothaan
Department of Physics
Chicago, Illinois

University of Florida
Attn: Dr. Alex Green
Physics Department
Gainesville, Florida

University of Michigan
Attn: Dr. R. Bernstein
Chemistry Department
Ann Arbor, Michigan

University of Michigan
Attn: Dr. Otto LaPorte
Physics Department
Ann Arbor, Michigan

University of Minnesota
Attn: Prof. H. J. Oskam
Department of Electrical
Engineering
Institute of Technology
Minneapolis 14, Minnesota
University of Pittsburgh
Attn: Prof. Wade Fite
Pittsburgh, Pa.

University of Southern Calif.
Attn: Prof. Gerhard L. Weissle
Dept. of Physics
University Park
Los Angeles 7, California

Westinghouse Electric Corp.
Attn: Dr. A. Phelps
Research Physicists
Research Laboratories
Pittsburgh 35, Pa.